

# Possible dark matter annihilation signal in the AMS-02 antiproton data

Ming-Yang Cui<sup>a,b</sup>, Qiang Yuan<sup>a,c\*</sup>, Yue-Lin Sming Tsai<sup>b,d</sup>, and Yi-Zhong Fan<sup>a,c†</sup>

<sup>a</sup>Key Laboratory of Dark Matter and Space Astronomy, Purple Mountain Observatory,  
Chinese Academy of Sciences, Nanjing 210008, P.R.China

<sup>b</sup>Department of Physics, Nanjing University, Nanjing 210093, P.R.China

<sup>c</sup>School of Astronomy and Space Science, University of Science and Technology of China, Hefei, Anhui 230026, P.R.China

<sup>d</sup>Physics Division, National Center for Theoretical Sciences, Hsinchu, Taiwan

(Dated: March 9, 2022)

Using the latest AMS-02 cosmic ray antiproton flux data, we search for potential dark matter annihilation signal. The background parameters about the propagation, source injection, and solar modulation are not assumed *a priori*, but based on the results inferred from the recent B/C ratio and proton data measurements instead. The possible dark matter signal is incorporated into the model self-consistently under a Bayesian framework. Compared with the astrophysical background only hypothesis, we find that a dark matter signal is favored. The rest mass of the dark matter particles is  $\sim 20 - 80$  GeV and the velocity-averaged hadronic annihilation cross section is about  $(0.2 - 5) \times 10^{-26} \text{ cm}^3 \text{ s}^{-1}$ , in agreement with that needed to account for the Galactic center GeV excess and/or the weak GeV emission from dwarf spheroidal galaxies Reticulum 2 and Tucana III. Tight constraints on the dark matter annihilation models are also set in a wide mass region.

PACS numbers: 95.35.+d, 96.50.S-

**Introduction** — The precise measurements of cosmic ray (CR) anti-particle spectra by space-borne instruments, such as PAMELA and AMS-02, provide very good sensitivity to probe the particle dark matter (DM) annihilation or decay in the Milky Way. The CR antiprotons, primarily come from the inelastic collisions between the CR protons (and Helium) and the interstellar medium (ISM), are effective to constrain the DM models [1–3]. Recent observations of the antiproton fluxes [4–6] are largely consistent with the expectation from the CR propagation model, leaving very limited room for the annihilation or decay of DM [2, 7–10].

There are several sources of uncertainties in using antiprotons to constrain DM models. The largest uncertainty may come from the propagation parameters. Usually the secondary-to-primary ratio of CR nuclei, such as the Boron-to-Carbon ratio (B/C), and the radioactive-to-stable isotope ratio of secondary nuclei, such as the Beryllium isotope ratio  $^{10}\text{Be}/^9\text{Be}$ , are used to determine the propagation parameters [11, 12]. Limited by the data quality, the constraints on the propagation parameters are loose [13, 14]. Even the effect on the background antiproton flux due to uncertainties of propagation parameters is moderate, the flux from the DM component depends sensitively on propagation parameters [15]. Additional uncertainties include the injection spectrum of the CR nuclei, solar modulation, and hadronic interaction models [8]. Those uncertainties make the DM searches with antiprotons inconclusive [16, 17].

Given the new measurements of the proton, Helium, and B/C data by PAMELA and AMS-02 [18–21], improved constraints on the propagation and source injection parameters can be obtained through global Bayesian approaches [22–25]. With these data, we conduct a global study to determine the propagation, injection, and solar modulation parameters si-

multaneously using the Markov Chain Monte Carlo (MCMC) method [26]. These “background” parameters and their likelihoods can be incorporated in the study of the DM model parameters by means of the Bayesian theorem, giving self-consistent and unbiased judgement of the DM models (see earlier attempts [17, 23]). In this work we apply this method to the most recently reported antiproton fluxes measured by AMS-02 [6]. Furthermore, we improve the constraints on the solar modulation parameters with the time-dependent proton fluxes measured by PAMELA [27]. Note, however, we adopt a relatively simple one-zone diffusion model in this work. It is possible that in reality the ISM and CR propagation are more complicated, e.g., vary everywhere [25].

**Background** — Here we simply introduce the fitting procedure to determine the propagation, injection, and solar modulation parameters [26, 28]. Hereafter they are referred to as background parameters. We work in the diffusion reacceleration<sup>1</sup> framework of the CR propagation, which was found to reproduce the peak of the B/C data around 1 GeV/n well [29]. The injection spectrum of nuclei is assumed to be a broken power-law with respect to rigidity. Although the spectrum of Helium (and heavier nuclei) is found to be harder than that of protons, we assume a unified set of injection parameters of all nuclei. Such an assumption is expected to not sensitively affect the calculation of the B/C ratio. The solar modulation model is adopted to be the force-field approximation [30]. As for the modulation potential, we employ a time-variation form  $\Phi = \Phi_0 + \Phi_1 \times \tilde{N}(t)$  to connect the modulation with solar activities which are characterized by the sunspot number<sup>2</sup>  $\tilde{N}(t)$  (normalized to 1 at solar maximum of cycle 24). The data used in the fitting include the B/C data by ACE [31] and AMS-

\*The corresponding author: yuanq@pmo.ac.cn

†The corresponding author: yzf@pmo.ac.cn

<sup>1</sup> Other propagation scenarios, such as the plain diffusion and diffusion convection models, have also been discussed in [26]. However, the diffusion reacceleration scenario is found to be best consistent with the data.

<sup>2</sup> <http://solarscience.msfc.nasa.gov/SunspotCycle.shtml>

02 [21], the proton spectrum by AMS-02 [19] and the time-dependent proton fluxes by PAMELA [27]. The  $^{10}\text{Be}/^9\text{Be}$  ratio is not well measured yet. We use some old data in the fitting (see Ref. [26]).

The numerical tool GALPROP [32, 33] is adopted to calculate the propagation of CRs. We have developed a global fitting tool, CosRayMC, which incorporates GALPROP into the MCMC sampler [34], enabling efficient survey of the high-dimensional parameter space of the CR propagation [35, 36]. Once the background parameters are obtained, the secondary production of antiprotons can be obtained, as shown in Fig. 1. Note that there are uncertainties from the antiproton production cross section [37–41]. Especially it has been found that an asymmetry exists between the antineutron and antiproton production for  $pp$  collisions, which tends to give more antineutrons [43]. An energy-independent rescaling factor of  $\kappa \simeq 1.3 \pm 0.2$  has been suggested to approximate the ratio of antineutron-to-antiproton production cross sections [39]. The energy-dependence of  $\kappa$  is unclear at present [39, 40]. We expect that a constant factor is a simple and reasonable assumption. For the results shown in Fig. 1 we adopt  $\kappa = 1.2$ .

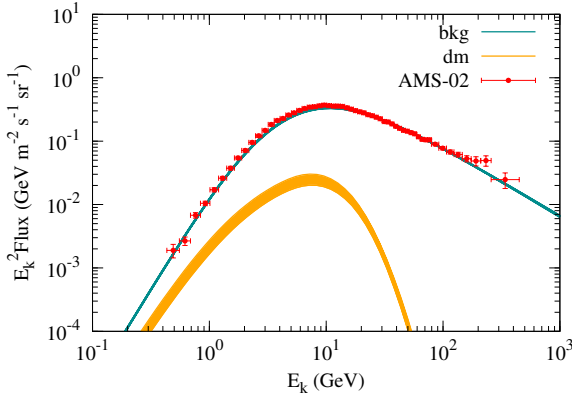


FIG. 1: Secondary and DM annihilation antiproton fluxes calculated for  $2\sigma$  ranges of the background parameters determined in the fitting to the B/C,  $^{10}\text{Be}/^9\text{Be}$ , and proton data. As an illustration, the mass of the DM particle is 47 GeV, the cross section is  $10^{-26} \text{ cm}^3 \text{ s}^{-1}$ , and the annihilation channel is  $b\bar{b}$ .

**DM annihilation** — Antiprotons can also be produced via the DM annihilation or decay. In this work we focus on the discussion of DM annihilation. The density profile of DM is adopted to be NFW profile [44],  $\rho(r) = \rho_s \left[ (r/r_s)(1 + r/r_s)^2 \right]^{-1}$ , where  $r_s = 20 \text{ kpc}$  and  $\rho_s = 0.26 \text{ GeV cm}^{-3}$ . The production spectrum of antiprotons is calculated using the tables given in [45]. Fig. 1 shows the results of DM induced antiproton fluxes, for  $m_\chi = 47 \text{ GeV}$  and  $\langle\sigma v\rangle = 10^{-26} \text{ cm}^3 \text{ s}^{-1}$  (for illustration), and various background parameters which lie in the  $2\sigma$  ranges derived in the background fitting. Due to the improved constraints on the propagation parameters (e.g., the half height of the propagation halo  $z_h = 5.9 \pm 1.1 \text{ kpc}$  [28]), the DM annihilation induced antiproton fluxes are constrained in a range of  $\sim 2$ , which improve much compared with previous studies (e.g., [15, 23]).

**Results of DM constraints** — From the Bayesian theorem, one can always update the prior from independent measurements. The posterior probability density of the parameter  $\langle\sigma v\rangle$  for given mass of the DM particle  $m_\chi$  can be written as

$$\mathcal{P}(\langle\sigma v\rangle)|_{m_\chi} \propto \int \mathcal{L}(m_\chi, \langle\sigma v\rangle, \theta_{\text{bkg}}, \kappa) p(\theta_{\text{bkg}}) p(\kappa) d\theta_{\text{bkg}} d\kappa,$$

where  $\mathcal{L}$  is the likelihood function of model parameters  $(m_\chi, \langle\sigma v\rangle, \theta_{\text{bkg}}, \kappa)$  calculated from the AMS-02 antiproton data,  $p(\theta_{\text{bkg}})$  is the prior of background parameters  $\theta_{\text{bkg}}$  which is obtained via the MCMC fitting to the B/C,  $^{10}\text{Be}/^9\text{Be}$ , and proton data, and  $p(\kappa)$  is the prior of the antineutron-to-antiproton production ratio, which is assumed to be Gaussian distribution  $N(1.3, 0.2^2)$  [39, 43].

We find that the AMS-02 data favor a DM component with a mass of a few tens GeV and an annihilation cross section of the thermal production level for quark final state. This conclusion holds for different antiproton production cross sections given in Refs. [37–39], as well as different source distributions of CRs [46]. The logarithmic Bayes factor value ( $2 \ln K$ ) of the DM component is found to be about 11 – 54 for the three cross section parameterizations used. The best fit DM mass is about 40 – 60 GeV, and the annihilation cross section is about  $(1 - 3) \times 10^{-26} \text{ cm}^3 \text{ s}^{-1}$  for  $b\bar{b}$  channel. Fig. 2 shows the favored parameter regions on the  $m_\chi - \langle\sigma v\rangle$  plane. For DM annihilation into  $W^+ W^-$ , similar results can be found with slightly heavier masses (due to the mass threshold to produce  $W$  bosons). Using the PAMELA data, Ref. [17] obtained similar results, although in a suggestive way with significantly larger uncertainties.

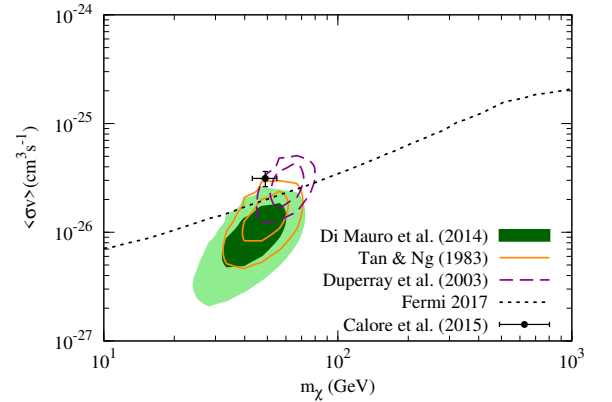


FIG. 2: Shaded regions and contours are the 68% and 95% credible regions of parameters  $m_\chi - \langle\sigma v\rangle$  to fit the antiproton data, for three parameterizations of the antiproton production cross sections [37–39]. The annihilation channel is assumed to be  $b\bar{b}$ . Also shown are the Fermi-LAT exclusion limits from observations of dwarf spheroidal galaxies [52], and the best-fit parameters (with a re-scaling of the local density) through fitting to the Galactic center GeV excess [53].

It is interesting to note that such a favored parameter region is consistent with that to fit the GeV  $\gamma$ -ray excess in the Galactic center region [54, 55], as well as the tentative  $\gamma$ -ray excesses in the directions of two dwarf galaxies [56, 57].

Also we find that the favored DM mass is consistent with that inferred from a tentative  $\gamma$ -ray line-like signal with energies  $\sim 43$  GeV from a population of clusters of galaxies [58]. Such a consistency, if not solely due to coincidence, strongly supports the common DM origin of the antiproton “anomaly” and GeV  $\gamma$ -ray excesses.

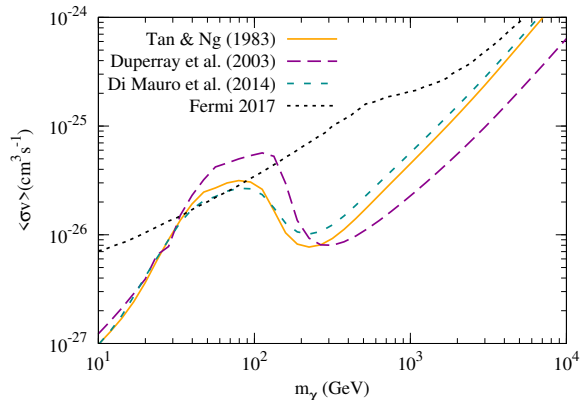


FIG. 3: The 95% credible upper limits of the DM annihilation cross section versus mass derived through fitting to the AMS-02 data, compared with that from Fermi-LAT observations of dwarf spheroidal galaxies [52].

We also derive the upper limits of the DM annihilation cross section for DM masses of  $10 - 10^4$  GeV, as shown in Fig. 3. Here the 95% credible limit of  $\langle\sigma v\rangle$  is obtained by setting  $\left(\int_0^{\langle\sigma v\rangle} \mathcal{P}(x)dx\right) / \left(\int_0^\infty \mathcal{P}(x)dx\right) = 0.95$ . Compared with that derived from the combined analysis of the Fermi-LAT  $\gamma$ -ray emission from a population of dwarf spheroidal galaxies [52], our limits are in general stronger, except for the mass range of  $30 - 150$  GeV where we find signal favored by the antiproton data. The DM density profiles may affect our constraints by a factor of  $\lesssim 2$ , for the Einasto or isothermal profile [23]. On the other hand, the local density adopted in this work,  $0.3 \text{ GeV cm}^{-3}$ , may be lower than that from recent kinematics measurements [59], which makes our constraints more conservative.

**Conclusion** — Compelling evidence indicates that DM particles consist of a substantial fraction of the energy density of the Universe. It is also widely anticipated that these exotic particles can annihilate with each other and produce stable high energy particle pairs, including for example electrons/positrons, protons/antiprotons, neutrinos/anti-neutrinos and  $\gamma$ -rays. However, so far no solid evidence for DM annihilation has been reported, yet.

In this work we use the precise measurement of the an-

tiproton flux by AMS-02 to probe the DM annihilation signal. The CR propagation parameters, proton injection parameters, and the solar modulation parameters, which are derived through independent fitting to the B/C and  $^{10}\text{Be}/^9\text{Be}$  ratios, and the time-dependent proton fluxes, are taken into account in the posterior probability calculation of the DM parameters self-consistently within the Bayesian framework. Such an approach does not assume background parameters in advance, and thus tends to give less biased results of the DM searches.

We find that the antiproton data suggest the existence of a DM signal. The favored mass of DM particles ranges from 20 to 80 GeV, and the annihilation cross section is about  $(0.2 - 5) \times 10^{-26} \text{ cm}^3\text{s}^{-1}$ , for  $b\bar{b}$  channel. Though further studies are still needed to firmly establish the DM origin of the antiproton “anomaly”, we notice that the inferred DM parameters are well consistent with that found in the modeling of the Galactic center GeV excess and/or the weak GeV emission in the directions of Reticulum 2 and Tucana III. Such a remarkable consistency, if not due to coincidence, points towards a common DM annihilation origin of these signals. The indication of a similar signal from various targets and different messengers will be very important for the search for particle DM. For other possibilities to explain the current puzzle please see [60]. We keep in mind that the current framework of the CR propagation is relatively simple. More detailed model may be necessary for future improvement of the understanding of this problem.

We have obtained the upper limits on the DM annihilation cross section from the antiproton data, which are stronger than that set by the Fermi-LAT observations of a population of dwarf spheroidal galaxies in a wide mass range. The improvement of constraints is expected to be beneficial from more precise measurements of the data by AMS-02, which reduce the uncertainties of both the background and the expectation of the signal. Our improved method also helps because the background parameters are taken into account with proper likelihood instead of a choice by hand.

*Note:* — Recently, Ref. [64] appears on arXiv. We have different approaches but consistent results.

## Acknowledgments

This work is supported in part by the National Basic Research Program of China (No. 2013CB837000), the National Key Research and Development Program of China (No. 2016YFA0400200), the National Natural Science Foundation of China (No. 11525313), and the 100 Talents program of Chinese Academy of Sciences.

- 
- [1] L. Bergström, J. Edsjö, M. Gustafsson, and P. Salati, *J. Cosmol. Astropart. Phys.* **5**, 006 (2006), astro-ph/0602632.
  - [2] F. Donato, D. Maurin, P. Brun, T. Delahaye, and P. Salati, *Phys. Rev. Lett.* **102**, 071301 (2009), 0810.5292.
  - [3] M. Cirelli, D. Gaggero, G. Giesen, M. Taoso, and A. Urbano, *J.*

- Cosmol. Astropart. Phys.* **12**, 045 (2014), 1407.2173.
- [4] O. Adriani, et al., *Phys. Rev. Lett.* **102**, 051101 (2009), 0810.4994.
- [5] O. Adriani, et al., *Phys. Rev. Lett.* **105**, 121101 (2010), 1007.0821.

- [6] M. Aguilar, et al., Phys. Rev. Lett. **117**, 091103 (2016).
- [7] N. Fornengo, L. Maccione, and A. Vittino, J. Cosmol. Astropart. Phys. **4**, 003 (2014), 1312.3579.
- [8] G. Giesen, M. Boudaud, Y. Génolini, V. Poulin, M. Cirelli, P. Salati, and P. D. Serpico, J. Cosmol. Astropart. Phys. **9**, 023 (2015), 1504.04276.
- [9] H.-B. Jin, Y.-L. Wu, and Y.-F. Zhou, Phys. Rev. D **92**, 055027 (2015), 1504.04604.
- [10] S.-J. Lin, X.-J. Bi, P.-F. Yin, and Z.-H. Yu, ArXiv e-prints (2015), 1504.07230.
- [11] T. K. Gaisser, *Cosmic rays and particle physics* (Cambridge and New York, Cambridge University Press, 1990, 292 p., 1990).
- [12] A. W. Strong, I. V. Moskalenko, and V. S. Ptuskin, Annual Review of Nuclear and Particle Science **57**, 285 (2007), astro-ph/0701517.
- [13] D. Maurin, F. Donato, R. Taillet, and P. Salati, Astrophys. J. **555**, 585 (2001).
- [14] A. Putze, L. Derome, and D. Maurin, Astron. Astrophys. **516**, A66 (2010), 1001.0551.
- [15] F. Donato, N. Fornengo, D. Maurin, P. Salati, and R. Taillet, Phys. Rev. D **69**, 063501 (2004), astro-ph/0306207.
- [16] T. Bringmann, M. Vollmann, and C. Weniger, Phys. Rev. D **90**, 123001 (2014), 1406.6027.
- [17] D. Hooper, T. Linden, and P. Mertsch, J. Cosmol. Astropart. Phys. **3**, 021 (2015), 1410.1527.
- [18] O. Adriani, et al., Science **332**, 69 (2011), 1103.4055.
- [19] M. Aguilar, et al., Phys. Rev. Lett. **114**, 171103 (2015).
- [20] M. Aguilar, et al., Phys. Rev. Lett. **115**, 211101 (2015).
- [21] M. Aguilar, et al., Phys. Rev. Lett. **117**, 231102 (2016).
- [22] R. Trotta, G. Jóhannesson, I. V. Moskalenko, T. A. Porter, R. Ruiz de Austri, and A. W. Strong, Astrophys. J. **729**, 106 (2011), 1011.0037.
- [23] H.-B. Jin, Y.-L. Wu, and Y.-F. Zhou, J. Cosmol. Astropart. Phys. **9**, 049 (2015), 1410.0171.
- [24] M. Korsmeier and A. Cuoco, Phys. Rev. D **94**, 123019 (2016), 1607.06093.
- [25] G. Jóhannesson, et al., Astrophys. J. **824**, 16 (2016), 1602.02243.
- [26] Q. Yuan, S.-J. Lin, K. Fang, and X.-J. Bi, Phys. Rev. D **95**, 083007 (2017), 1701.06149.
- [27] O. Adriani, et al., Astrophys. J. **765**, 91 (2013), 1301.4108.
- [28] See Supplemental Material A.
- [29] I. V. Moskalenko, A. W. Strong, J. F. Ormes, and M. S. Potgieter, Astrophys. J. **565**, 280 (2002), astro-ph/0106567.
- [30] L. J. Gleeson and W. I. Axford, Astrophys. J. **154**, 1011 (1968).
- [31] J. S. George, et al., Astrophys. J. **698**, 1666 (2009).
- [32] A. W. Strong and I. V. Moskalenko, Astrophys. J. **509**, 212 (1998), astro-ph/9807150.
- [33] I. V. Moskalenko and A. W. Strong, Astrophys. J. **493**, 694 (1998), astro-ph/9710124.
- [34] A. Lewis and S. Bridle, Phys. Rev. D **66**, 103511 (2002), astro-ph/0205436.
- [35] J. Liu, Q. Yuan, X. J. Bi, H. Li, and X. M. Zhang, Phys. Rev. D **81**, 023516 (2010), 0906.3858.
- [36] J. Liu, Q. Yuan, X.-J. Bi, H. Li, and X. Zhang, Phys. Rev. D **85**, 043507 (2012), 1106.3882.
- [37] L. C. Tan and L. K. Ng, Journal of Physics G Nuclear Physics **9**, 1289 (1983).
- [38] R. P. Duperray, C.-Y. Huang, K. V. Protasov, and M. Buénerd, Phys. Rev. D **68**, 094017 (2003), astro-ph/0305274.
- [39] M. di Mauro, F. Donato, A. Goudelis, and P. D. Serpico, Phys. Rev. D **90**, 085017 (2014), 1408.0288.
- [40] R. Kappl and M. W. Winkler, J. Cosmol. Astropart. Phys. **9**, 051 (2014), 1408.0299.
- [41] See Supplemental Material B, which includes Ref. [42].
- [42] M. Kachelriess, I. V. Moskalenko, and S. S. Ostapchenko, Astrophys. J. **803**, 54 (2015), 1502.04158.
- [43] H. G. Fischer and NA49 Collaboration, Acta Physica Hungarica Heavy Ion Physics **17**, 369 (2003).
- [44] J. F. Navarro, C. S. Frenk, and S. D. M. White, Astrophys. J. **490**, 493 (1997), astro-ph/9611107.
- [45] M. Cirelli, G. Corcella, A. Hektor, G. Hütsi, M. Kadastik, P. Panci, M. Raidal, F. Sala, and A. Strumia, J. Cosmol. Astropart. Phys. **3**, 051 (2011), 1012.4515.
- [46] See Supplemental Material C, which includes Ref. [47-51].
- [47] M. Ackermann, et al., Astrophys. J. **750**, 3 (2012).
- [48] D. R. Lorimer, et al., Mon. Not. Roy. Astron. Soc. **372**, 777 (2006), astro-ph/0607640.
- [49] I. Yusifov and I. Küçük, Astron. Astrophys. **422**, 545 (2004), astro-ph/0405559.
- [50] G. L. Case and D. Bhattacharya, Astrophys. J. **504**, 761 (1998), astro-ph/9807162.
- [51] L. Bronfman, S. Casassus, J. May, and L.-Å. Nyman, Astron. Astrophys. **358**, 521 (2000), astro-ph/0006104.
- [52] A. Albert, et al., Astrophys. J. **834**, 110 (2017).
- [53] F. Calore, I. Cholis, and C. Weniger, J. Cosmol. Astropart. Phys. **3**, 038 (2015), 1409.0042.
- [54] D. Hooper and L. Goodenough, Physics Letters B **697**, 412 (2011), 1010.2752.
- [55] K. N. Abazajian and M. Kaplinghat, Phys. Rev. D **86**, 083511 (2012), 1207.6047.
- [56] A. Geringer-Sameth, M. G. Walker, S. M. Koushiappas, S. E. Koposov, V. Belokurov, G. Torrealba, and N. W. Evans, Phys. Rev. Lett. **115**, 081101 (2015), 1503.02320.
- [57] S. Li, Y.-F. Liang, K.-K. Duan, Z.-Q. Shen, X. Huang, X. Li, Y.-Z. Fan, N.-H. Liao, L. Feng, and J. Chang, Phys. Rev. D **93**, 043518 (2016), 1511.09252.
- [58] Y.-F. Liang, Z.-Q. Shen, X. Li, Y.-Z. Fan, X. Huang, S.-J. Lei, L. Feng, E.-W. Liang, and J. Chang, Phys. Rev. D **93**, 103525 (2016), 1602.06527.
- [59] P. Salucci, F. Nesti, G. Gentile, and C. Frigerio Martins, Astron. Astrophys. **523**, A83 (2010), 1003.3101.
- [60] See Supplemental Material D, which includes Ref. [61-63].
- [61] V. A. Dogiel, A. V. Gurevich, I. N. Istomin, and K. P. Zybin, Mon. Not. Roy. Astron. Soc. **228**, 843 (1987).
- [62] I. V. Moskalenko, A. W. Strong, S. G. Mashnik, and J. F. Ormes, Astrophys. J. **586**, 1050 (2003), astro-ph/0210480.
- [63] G. di Bernardo, C. Evoli, D. Gaggero, D. Grasso, and L. Maccione, Astroparticle Physics **34**, 274 (2010), 0909.4548.
- [64] A. Cuoco, M. Kramer, and M. Korsmeier, Phys. Rev. Lett. **118**, 191102 (2017), 1610.03071.



## Supplemental Material

### A. Background parameters

The background parameters used to calculate the secondary antiproton fluxes include the propagation, source spectra, and solar modulation parameters. The major propagation parameters are: the rigidity-dependent diffusion coefficient  $D(R) = \beta D_0 (R/4 \text{ GV})^\delta$  where  $R$  is the rigidity of a particle and  $\beta$  is the velocity in unit of speed of light, the half-height of the propagation halo  $z_h$ , and the Alfvénic speed  $v_A$  which characterizes the reacceleration. The injection spectrum of CR nuclei is assumed to be a broken power-law in rigidity, with indices  $\nu_1$  and  $\nu_2$  below/above the break rigidity  $R_{br}$ . The post-propagated proton flux is normalized to  $A_p$ . The spatial distribution of CR sources is parameterized as

$$f(r, z) = (r/r_s)^{1.25} \exp[-3.56(r - r_s)] \exp(-|z|/z_s),$$

where  $r_s = 8.5 \text{ kpc}$  and  $z_s = 0.2 \text{ kpc}$ . Such a distribution follows the pulsar distribution with parameters adjusted slightly based on the diffuse  $\gamma$ -ray data [22]. Finally, there are two solar modulation parameters,  $\Phi_0$  and  $\Phi_1$ , as described in the main text. The parameters values obtained in the MCMC fittings of Ref. [26] are given in Table I.

TABLE I: Mean values and posterior  $1\sigma$  uncertainties of the parameters for the fitting with B/C,  $^{10}\text{Be}/^9\text{Be}$ , and the proton spectra.

Parameter	Unit	Value
$D_0$	$(10^{28} \text{ cm}^2 \text{ s}^{-1})$	$7.24 \pm 0.97$
$\delta$		$0.380 \pm 0.007$
$z_h$	(kpc)	$5.93 \pm 1.13$
$v_A$	$(\text{km s}^{-1})$	$38.5 \pm 1.3$
$\log(A_p^a)$		$-8.347 \pm 0.002$
$\nu_1$		$1.69 \pm 0.02$
$\nu_2$		$2.37 \pm 0.01$
$\log(R_{br}^b)$		$4.11 \pm 0.02$
$\Phi_0$	(MV)	$180 \pm 8$
$\Phi_1$	(MV)	$487 \pm 11$

Notes: <sup>a</sup>Propagated flux normalization of protons at 100 GeV in unit of  $\text{cm}^{-2} \text{s}^{-1} \text{sr}^{-1} \text{MeV}^{-1}$ . <sup>b</sup>Break rigidity of the proton injection spectrum in unit of MV.

### B. Hadronic $pp$ interactions

There are relatively large uncertainties of the hadronic interaction models of inelastic  $pp$  collisions. The default model of this work uses the parameterization given by Tan & Ng [37]. With more and more experimental data, updated parameterizations were available in literature [38–40]. Note further that there are heavy nuclei in both the CRs and the ISM. A nuclear enhancement factor from Monte Carlo simulations,  $\epsilon = 1.58 \times (E_k/\text{GeV})^{0.034}$ , is employed [42]. In the left panel of Fig. 4 we show the comparison of results for several different parameterizations of antiproton production from  $pp$ -collision.

We find that there are several tens percents difference between each other. However, the qualitative conclusion that there are low energy deficits of antiprotons compared with the AMS-02 data keeps unchanged. The logarithmic Bayes factor of adding a DM component to the background model, is about 19 for cross sections of Ref. [37], 54 for Ref. [38], and 11 for Ref. [39]. Note that we use Eq. (12) in Ref. [39] in this work. Another formula (Eq. (13)) was also given in Ref. [39]. Using Eq. (13) we find that the background antiproton flux is overall lower by a factor of  $\sim 1.35$  than the data, but no significant DM signal is shown. The problem is that Eq. (13) may give unrealistic extrapolation of the results out of the energy coverage by the data which is about 4 – 500 GeV, due to a cubic term of the  $p_T$ -dependence [39]. Also the spline interpolation method in Ref. [39] gives similar result as that of Eq. (12) in the energy range we are mostly interested in (GeV to tens of GeV).

The right panel of Fig. 4 shows ratios of data to model predictions of antiproton fluxes for the three  $pp$  interaction parameterizations. It is clear to show that there are all low energy excesses of the data compared with the predictions, even when a constant rescaling factor  $\kappa$  is applied to the models. In particular, the excesses can not be simply ascribed to the uncertainties of the parameterizations, as illustrated by the shaded region for that of Ref. [39].

### C. Test of CR source distributions

The origin of CRs is still in debate, and hence the source distributions of CRs are essentially unknown. Here we test the effect of different source distributions. We consider the four kinds of radial distributions which were discussed in Ref. [47] to fit the diffuse  $\gamma$ -ray data of Fermi-LAT. They are: two parameterizations of pulsar distributions [48,49], supernova remnant (SNR) distribution [50], and the massive OB star distribution [51]. Also we know that there are spiral structures of stars and gas in the Galaxy. We thus employ a sinusoidal radial distribution function,  $f(r) = 1 + \sin(r/0.67 \text{ kpc})$ , to mimic the spiral arm-like distribution of CR sources. The  $z$ -direction distribution is adopted to be  $\propto \exp(-|z|/0.2 \text{ kpc})$  for all source functions. For each source distribution, the background parameters are identical to the mean values given in Table I, except for  $D_0$  which is slightly adjusted to match the B/C data. As shown in Fig. 5, different source distributions lead to very little difference of both the B/C ratios and antiproton fluxes.

### D. Astrophysical interpretations

It is interesting to investigate whether there are astrophysical sources other than the DM annihilation, which can produce the excess antiprotons without violating the B/C data. Generally speaking, an astrophysical source (for instance, SNR) will produce secondary antiprotons and nuclei simultaneously. We consider such an “X” component, assuming the same source parameters as the background CRs except that an exponential cutoff with characteristic rigidity of 30 GeV is assumed, in or-

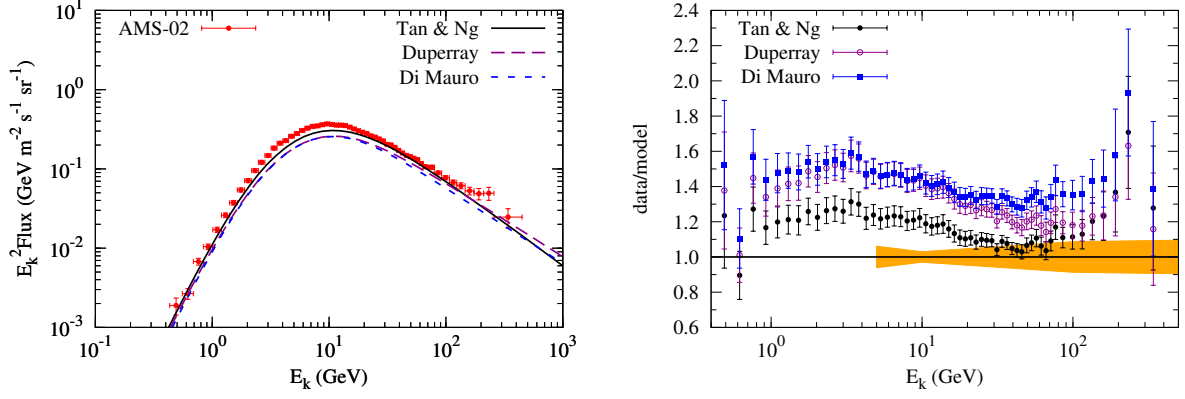


FIG. 4: Left: antiproton fluxes for different parameterizations of  $pp$  collision induced antiproton yield spectra. Right: ratios of data to model predictions for different  $pp$  interaction parameterizations. The shaded region shows the uncertainty bands of the parameterization given in Ref. [39]. In this plot  $\kappa = 1$  is assumed.

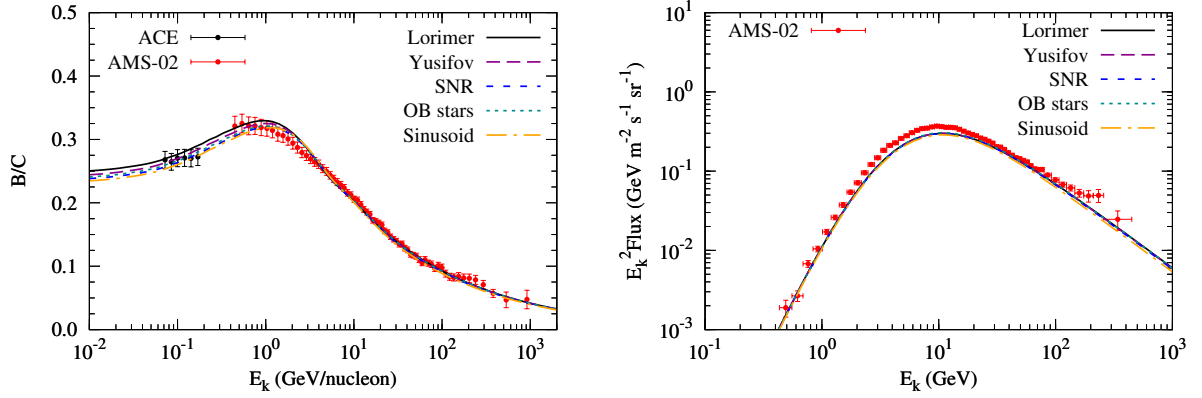


FIG. 5: The B/C ratios (left) and antiproton fluxes (right) for different source distributions: pulsars from Lorimer et al. [48], pulsars from Yusifov & Kucuk [49], supernova remnants [50], OB stars [51], and a sinusoid function.

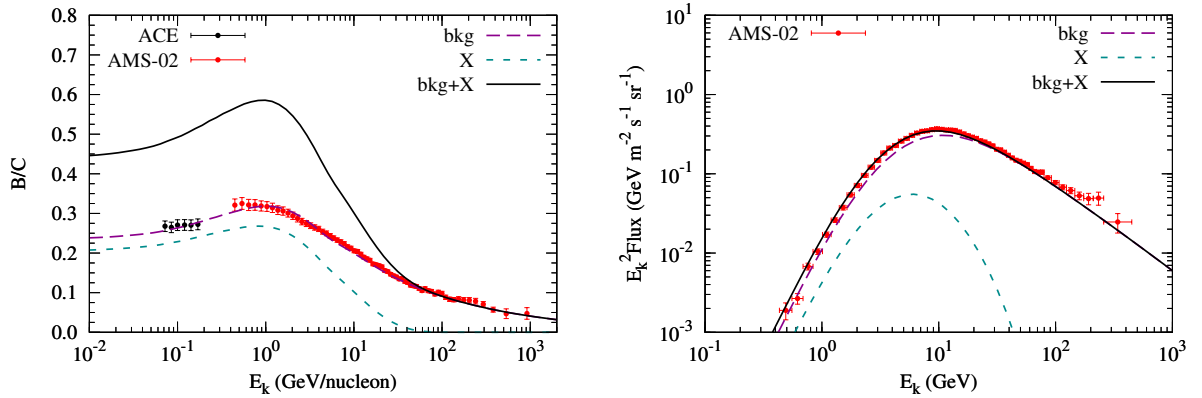


FIG. 6: The B/C ratio (left) and antiproton flux (right) for the model with an astrophysical component “X”.

der to fit the antiproton data. Also we assume that this “X” component contributes negligible primary CRs. A potential astrophysical realization is the acceleration and interaction of

CRs within molecular clouds [61]. Fig. 6 shows the results for the scenario with such an “X” component. We find that to produce proper amount of antiprotons, the model over-produces

Boron nuclei by a factor of  $\sim 2$ . Only if the relative abundance of Carbon/Oxygen to protons is a factor of about 30 lower than that of the background sources, the model can simultaneously account for the antiproton and B/C data. Note that the “X-to-bkg” ratio of antiprotons is smaller than that of the B/C ratio. This is because antiprotons are produced by parent protons with much higher energies which are suppressed due to the cutoff of primary CRs for the “X” component. We have tested that when the cutoff rigidity approaches infinity, the “X-to-bkg” ratio of antiprotons asymptotically approaches that of the B/C.

An alternative astrophysical scenario to reconcile the antiproton and B/C data was proposed in Ref. [62], in which a local and fresh source (perhaps associated with the local bubble) is postulated to contribute additional low energy primaries and decrease the measured secondary/primary ratio. Since the local source will also produce protons, the injection spectrum of the Galactic component of protons need to be significantly suppressed below several GeV. This may not affect the antiproton production due to a high threshold energy, but may imprint in the diffuse  $\gamma$ -rays. Further studies of the consistency between the model prediction and the Fermi-LAT diffuse  $\gamma$ -ray data may be interesting to test the model.

In Ref. [63], the authors suggested an empirical adjustment of the diffusion coefficient with a velocity-dependent term  $\beta^\eta$  to explain the B/C and antiproton data. However, the physical reason for such an adjustment is not well justified.

We suggest that the DM annihilation scenario is a simple model that can reasonably reproduce the antiproton data. The inferred physical parameters are in agreement with several other hints from  $\gamma$ -ray observations of various targets. Therefore, it may be the time to seriously consider the possibility of their DM origin.